Rinne, Tommi; Saeed, Mohazzam; Serna-Guerrero, Rodrigo

Quantifying the degree of selectivity in a Flocculation-Flotation process of $LiCoO_2$ and graphite using scanning electron microscopy and image processing analysis

Published in:
Minerals Engineering

DOI:
10.1016/j.mineng.2024.108644

Published: 01/04/2024

Document Version
Publisher's PDF, also known as Version of record

Minerals Engineering 209 (2024) 108644

Contents lists available at ScienceDirect

Minerals Engineering

journal homepage: www.elsevier.com/locate/mineng

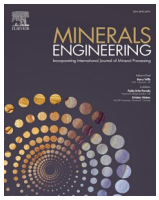

Quantifying the degree of selectivity in a Flocculation-Flotation process of $LiCoO_2$ and graphite using scanning electron microscopy and image processing analysis

Tommi Rinne, Mohazzam Saeed, Rodrigo Serna-Guerrero *

Department of Chemical and Metallurgical Engineering, School of Chemical Engineering, Aalto University, 02150 Espoo, Finland

ARTICLE INFO

Keywords:
Lithium-ion batteries
Direct recycling
Froth flotation
Selective flocculation
DBSCAN
Scanning electron microscopy

ABSTRACT

This research article studies selective flocculation as a means for improving flotation of lithium-ion battery active materials using mixtures of pure $LiCoO_2$ (LCO) and graphite. Scanning electron microscopy (SEM) combined with image analysis via density-based spatial clustering of applications with noise (DBSCAN) is presented as a novel method to quantitatively determine the degree of selectivity in a process that applies selective flocculation as a conditioning stage for froth flotation. SEM was shown to provide visual proof of flocculated particles, even in dried froth samples. Under optimal flocculant concentration of 10 g/t only a few flocs were detected in the froth concentrate, suggesting that heteroflocculation of LCO and graphite was minimized under said conditions. Using a flocculant concentration in excess (50 g/t) resulted in multiple flocculated LCO particles within the froth, indicating loss of flocculation selectivity. These results were corroborated by batch flotation experiments, which showed that treating the pulp with 10 g/t flocculant concentration yielded a graphite froth product at a grade of 98.2 %, compared to 98.1 % recovered from a non-flocculated pulp. An excess flocculant concentration led to a drastic reduction in graphite grade. Similar graphite recoveries were observed in all flotation experiments, indicating that the reduced graphite grade with excess flocculant was a result of hydrophobic heteroflocs carrying entrapped LCO to the froth. Proper pH control throughout the experiment prevented a negative influence of flocculation on the kinetics of graphite recovery, which had been reported in earlier research. The results suggest that selective flocculation is a potential method for improving the separation efficiency of graphite from Li-ion battery waste, and that SEM/DBSCAN can be applied for characterization of selectivity in combined flocculation-flotation processes.

1. Introduction

In the realm of contemporary energy systems, lithium-ion batteries (LIBs) have emerged as an indispensable power source technology, revolutionizing sectors ranging from portable electronics to electric vehicles (EVs) and grid-scale energy storage. LIBs present characteristics such as high energy density, longevity, and rechargeability that have propelled their widespread adoption. As the governments around the world pursue ambitious environmental and circular economy goals, the significance of recycling LIBs comes to the fore. For instance, the importance of recycling LIBs was recently highlighted in the Regulation on Batteries and Waste Batteries that adopted by the European Union in July 2023. This new regulation sets a target rate for end-of-life LIB collection (73 % by the end of 2031), element-specific recovery targets in LIB recycling processes (80 % for Li, 95 % for Co, Ni, and Cu by the end of 2031), and a mandatory minimum level of recycled content for newly manufactured EV batteries (16 % for Co, 6 % for Li and Ni) (European Commission 2023a). Moreover, the 2023 European Critical Raw Materials Regulation categorizes active materials for LIBs, namely Co, Ni, Li, Mn and graphite, as strategic raw materials, owing to their significance in the realm of green technology, and their inherent potential to pose supply chain vulnerabilities in the foreseeable future (European Commission 2023b). Among the strategic raw materials essential for LIBs, graphite stands as the only non-recoverable material in current industrial LIB recycling methodologies (hydrometallurgy and pyrometallurgy) (Beaudet et al., 2020). It is thus anticipated that the recycling of battery-grade graphite will gain significance in the upcoming years.

* Corresponding author.
E-mail addresses: tommi.rinne@aalto.fi (T. Rinne), mohazzam.saeed@aalto.fi (M. Saeed), rodrigo.serna@aalto.fi (R. Serna-Guerrero).

https://doi.org/10.1016/j.mineng.2024.108644
Received 16 October 2023; Received in revised form 20 February 2024; Accepted 28 February 2024
Available online 2 March 2024

In industrial LIB recycling processes, end-of-life batteries are processed mechanically to separate the active components into a fine-powder mixture commonly known as *"black mass"* (Harper et al., 2019). Recently, froth flotation of black mass has been studied by multiple authors as a potential separation process for the anode and cathode powders (Dańczak et al., 2021; Folayan et al., 2021; He et al., 2017; Huang, Han, Liu, et al., 2016; Liu et al., 2020; Rinne et al., 2022; Ruismäki et al., 2020; Salces et al., 2022; Saneie et al., 2022; Vanderbruggen et al., 2022; Yu et al., 2018; Zhang et al., 2021). The cathode material in LIBs is a Li-metal oxide, typically $LiCoO_2$ (LCO), $LiNi_xMn_yCo_zO_2$ (NMC), $LiNi_xCo_yAl_zO_2$, or $Li_xMn_yO_z$, while the anode is usually spherodized graphite (Chen et al., 2019; Velázquez-Martínez et al., 2019). The cathode oxides are commonly considered to have a hydrophilic character, whereas graphite is a naturally hydrophobic mineral. Due to this wettability gradient, flotation is considered a promising technology for separating graphite, either for direct recycling, or in preparation for the subsequent extraction of metallic species (e.g., Co, Ni, Li) via hydrometallurgical processes (Traore & Kelebek, 2022). Since graphite does not dissolve during leaching of black mass, the recycling operators often view it as an impurity – a component that can be tolerated but not recovered (Beaudet et al., 2020). However, the upstream separation of graphite has not been seen economically viable to the recycling operators, as most of the value in LIB recycling is generated by recovering the metals in the cathodic particles (Harper et al., 2019). Indeed, the monetary worth of cathode-grade (99.8 %) metals, specifically Co and Ni, surpasses that of graphite by a factor ranging from 10 to 100. The valuation of graphite primarily hinges on the purity and quality of the retrieved material, with battery-grade graphite (>99 % purity) representing the highest intrinsic worth (Brückner et al., 2020). In order for flotation-based recovery of graphite from LIB waste to be economically justified, it is thus anticipated that the recovery of the cathode components to the froth concentrate must be thoroughly minimized, with graphite grades above 99 % being preferable. However, it is noteworthy to point out that direct recycling via flotation also holds the potential to recover the cathodic Li-metal oxides in a form fit for purpose, maximizing the value of the recyclates in general.

A recent article published by the authors of this paper, demonstrated that achieving > 99 % graphite grades in black mass flotation will require optimizing the particle size of the cathode components (Rinne et al., 2023). A typical industrial NMC/LCO black mass contains a significant fraction of ultrafine particles, with d10 and d50 values of 2.7 μm, and 16.9 μm, respectively (Vanderbruggen et al., 2022). Such ultrafine particles tend to report non-selectively to the froth concentrate via entrainment, due to fluid drag forces as opposed to hydrophobic/hydrophilic interactions (Wang, Sun, & Liu, 2021; Wang, Wang, et al., 2021). In the context of black mass flotation, this phenomenon lowers the grade of the graphite concentrate, and its magnitude is proportional to the ultrafine cathode content of the black mass. To solve this issue, our research team recently published a study on selective cathode flocculation as a conditioning step prior to black mass flotation, in an attempt to increase the cathode particle size and minimize entrainment (Rinne et al., 2023).

In the aforementioned research article, increased graphite grades in froth concentrates were obtained when a feed of analytically pure graphite and LCO (a.k.a. *model black mass*) was conditioned with 20 g/t of a branched cationic polyacrylamide flocculant in pH 5. This result was regarded as indirect evidence of electrically selective flocculation of the cathode, and a proof-of-concept for the selective flocculation of LCO in mixtures with graphite. However, the consistent presence of cathode materials in the froth indicated the non-selective formation of heteroflocs. The paper hypothesized that the wettability nature of a heterofloc would be determined by its LCO-graphite ratio. After examining the grade-recovery data of graphite in each flocculation-flotation experiment, it was postulated that hydrophilic heteroflocs result in a lower graphite recovery, whereas hydrophobic heteroflocs are detrimental for graphite grade. However, characterization of floc structures was not provided, leaving room for speculation whether the observed alterations in grade-recovery data could be ascribed to heterofloc formation or if alternative factors were contributory. Competing hypothesis included, for example, selectivity loss induced by modifications in hydrodynamic conditions resulting from the application of the highly viscous flocculant polymer. It remained unresolved whether the formed flocs possessed the mechanical integrity to endure the vigorous forces exerted during agitation within the flotation cell, given that the laser diffraction measurements of particle size, used to monitor the formation of flocs, were conducted under conditions of lower mechanical mixing. The current paper aims to expand on this previously published research by showcasing a flocculation process with improved performance, rationalized with the support of floc structure characterization.

Firstly, the work hereby presented explores whether scanning electron microscopy (SEM) can be used as a methodology for qualitative characterization of selectivity in a combined flocculation-flotation process of battery materials. Such characterization is not trivial since flocs are bound together by polymers (*flocculants*) dissolved in aqueous media, whereas SEM requires dry samples for analysis. It is therefore necessary to establish whether flocs produced under the studied system possess sufficient mechanical integrity to be detected from carefully dried samples. In the context of LIB recycling, other authors have utilized SEM-EDS in the past to characterize black mass samples for particle morphology, particle liberation, and elemental content (Vanderbruggen et al., 2021). Furthermore, multiple articles discussing flocculation of natural minerals have presented SEM imaging as supportive characterization data (Cheng et al., 2022; Huang, Han, Liu, & Wang, 2016; Kumar & Mandre, 2017; Li et al., 2021; Li, 2022). In the specific case of articles discussing selective flocculation of mixed mineral dispersions, SEM-EDS characterization has been successfully applied to observe indirect evidence of flocculation selectivity based on, for example, desliming (Kumar & Mandre, 2017), particle clustering (Li et al., 2021), and detection of flocculant polymers on target mineral surfaces (Huang, Han, Liu, & Wang, 2016). Out of these techniques, particle clustering could arguably provide the best chance of visualizing the flocs. In the article of Li et al., SEM characterization was performed on mineral samples consisting of a 1:1 ratio of hematite and quartz that were subjected to asynchronous flocculation prior to imaging (Li et al., 2021). However, under such conditions, a relatively large quantity of multi-particle clusters consisting of similar minerals is expected to form by chance, making it difficult to distinguish between noise clusters and clusters that account for flocculated particles. The main advantage of the SEM characterization campaign conducted in the present article stems from the imaging of high purity (>90 %) graphite concentrates, in which the graphite matrix provides a visible contrast for potential LCO flocs, and the number of noise clusters is reduced. Deductions on the selectivity of flocculation can then be made following the postulates presented in the earlier work of the authors (Rinne et al., 2023).

To carry out a meaningful characterization, it is expected that dried LCO flocs will appear as particle clusters within SEM images taken from the froth concentrates. Mapping out the quantity and characteristics of such particle clusters could allow SEM to be utilized for the visualization of flocs and provide a better understanding on the degree of selectivity when battery material mixtures are flocculated in preparation for froth flotation. To minimize human bias in image analysis and to gather quantitative data on flocculation selectivity, machine learning data algorithms can be implemented to identify clusters and patterns. Developing and showcasing an algorithm capable of analyzing flocculation selectivity is the second objective of the present manuscript. Therefore, an unsupervised machine learning algorithm, density-based spatial clustering of applications with noise (DBSCAN), was used to categorize the particles in clusters based on their spatial distances. In their seminal work, Ester et al. (Ester et al., 1996) proposed this unsupervised clustering technique to address the challenges posed by irregularly dispersed data sets. DBSCAN is based on data density to classify clusters within the data sets disregarding the influence of distance and direction of the

clustering process (Mu et al., 2023). This distinguishing feature enables DBSCAN to precisely classify clusters in widely scattered data sets of arbitrary shapes. Owing to these features, DBSCAN has gained significant recognition as one of the foremost density-based clustering algorithms (Mu et al., 2023). In the specific case of this article, such methodology is applied to obtain quantitative data on the selectivity of flocculation, in addition to the qualitative data obtained from SEM. Based on the characterization results obtained, the limitations of selective flocculation can be rationalized, providing points for the optimization black mass separation.

2. Materials and methods

2.1. Materials

To produce the feed for the flocculation-flotation experiments, analytically pure $LiCoO_2$ (LCO) and spherodized graphite were mixed in a 1:1 ratio to obtain a mixture hereafter referred to as "model black mass". LCO (purity > 99.5 %) was purchased from MSE Supplies (Tucson, AZ, USA), and graphite (purity 99.95 %) was supplied by Pro-Graphite GmbH (Untergriesbach, Germany). Based on the particle size of the LCO used in this study, the abbreviation "LCO-M" (medium) was chosen for this material, to distinguish between the comparatively finer and coarser LCO samples used in previous studies.

A commercially available medium cationic branched polyacrylamide (CatPAM) flocculant with the trade name FO 4498 SSH (SNF Floerger Andrézieux, France) was used in this study and is hereby referred to as FO 4498.

The preparation of flocculant solutions involved the initial wetting of dry flocculant powder with ethanol in a 1:2 wt ratio, followed by one minute of vigorous manual mixing. Subsequently, ion-exchanged water was introduced to achieve flocculant dissolution at a specified concentration of 0.5 wt-%. For uniform dissolution of the polymer, the flocculant solutions underwent continuous stirring for 24 h using a magnetic stirrer. Prior to experimentation, the 0.5 wt-% mother solutions were further diluted to the desired concentrations. To maintain the integrity of the flocculant, each individual mother solution was utilized within 48 h of its initial preparation and subsequently discarded to mitigate potential degradation. Throughout the entire lifespan of the flocculant solution, continuous magnetic stirring was employed to uphold dissolution stability. In the flotation experiments, 0.1 M HCl (purity 99.5 %, Sigma-Aldrich, St. Louis, MO, USA) was applied as a pH regulator, and methyl isobutyl carbinol (MIBC, 98 % purity, Sigma-Aldrich) was used as a frother. Furthermore, sodium hexametaphosphate (SHMP, 96 % purity, Sigma-Aldrich) was applied as a graphite dispersant in selected experiments.

2.2. Experimental methods

2.2.1. Particle size measurements

The particle size distributions (PSDs) of non-flocculated ('pristine') and flocculated single mineral dispersions of LCO-M and graphite were assessed using a Malvern Mastersizer 3000 laser diffraction particle size analyzer (Malvern Panalytical Mastersizer 3000, Malvern, United Kingdom). PSD measurements, as well as the subsequent flotation experiments, were carried out in a target pH of 5. The target pH was chosen based on an observed zeta potential gradient between graphite and LCO particles under said conditions. For the interested reader, measurements of zeta potential for graphite and LCO are available in a previous publication from our research team (Rinne et al., 2023).

For flocculated samples, the following methodology for PSD measurements was employed: a measured amount of sample (within the range of 0.08–0.14 g) was dispersed in distilled water to achieve a pulp density of 40 g/L. The suspension's pH was adjusted to the target pH of 5 using 0.01 M HCl. Subsequently, the suspension was vigorously hand-mixed for 2 min, followed by the addition of a flocculant. To facilitate floc formation and growth, 3 min of vigorous mixing ensued. After conditioning, the flocculated suspension was transferred to a beaker containing 500 mL of water preadjusted to pH 5, and the measurement commenced. Table 1 provides the parameters for the PSD measurements.

Additionally, jar tests were conducted for suspensions of LCO-M, graphite, and model black mass, and sedimentation rates were monitored and measured. Jar tests were performed for both pristine suspensions and suspensions flocculated with 100 g/t of FO 4498. In the jar tests, a 1 g sample was first dispersed into 25 mL of distilled water (40 g/L pulp density), and the pH of the suspension adjusted with 0.01 M HCl to reach pH 5. Similar methodology, as described for PSD measurements, was then applied for mixing and conditioning of the sample. Once mixing and conditioning was finished, the sampling tubes were left undisturbed in a fume hood, and sedimentation rates were recorded.

2.2.2. Flotation

Flotation was carried out on model black mass samples treated with three concentrations of flocculant. Firstly, a baseline experiment with pristine (i.e., non-flocculated) black mass was performed. Secondly, an experiment was performed applying a flocculant concentration of 10 g/ton. Finally, flotation was performed with an excess amount of flocculant in the presence of a dispersant, to increase heteroflocculation for imaging purposes. To account for statistical variance in the flotation results and SEM imaging samples, experiments were replicated multiple times. Table 2 present the parameters in each flotation experiment performed in this study.

Batch flotation experiments were performed with a manually operated flotation device (Lab Cell—60 mm FloatForce mechanism, Outotec, Espoo, Finland) in a 1 L flotation cell. A total of 40 g of model black mass were fed to the cell, followed by the addition of 900 mL of ion-exchanged water. The pH was monitored with a FiveGo Portable F2 pH/mV meter ™ (Mettler Toledo, Greifensee, Switzerland). Sufficient 10^{-2} M HCl was then added to first reach a pH of 5, and the remaining liquid (10^{-5} M HCl) added after to obtain a solid–liquid ratio of ca. 40 g/L. The pulp was then agitated with an impeller at 1000 RPM for 3 min to ensure proper mixing before the addition of frother. Since the pH of the pulp was observed to increase during conditioning, it was monitored throughout conditioning, and 0.1 M HCl solution was added whenever necessary to maintain the pH between 5 and 6. In the experiment where a dispersant was used, the dispersant was added first, and conditioned for 3 min. After this, a flocculant was added, and the mixture was stirred for 3 min. Frother was added last with a conditioning period of 2 min. Throughout mixing and conditioning, the impeller rate was kept at 1000 RPM. Right before flotation started, the impeller rate was decreased to 850 RPM, and air was then allowed to flow at a rate of 2 L/min to the bottom of the cell via an outlet in the impeller.

The formation of froth started immediately after initialization of the airflow, marking the beginning of the experiment ($t_{0\ min}$). Froth collection was started after first allowing the froth surface to rise to a constant height. The first froth concentrate was collected during the first minute of the experiment ($t_{0–1\ min}$) by continuously scooping the froth into a container. The second froth concentrate was collected and placed in another container, by scooping 10 times/30 s during the timeframe t = 1—10 min, or as long as froth formation lasted. Throughout the experiment, the pH of the pulp was monitored and kept between 5 and 6 by adding 0.1 M HCl whenever necessary.

After flotation, the froth concentrates and flotation underflow were vacuum filtered and air dried in a convection oven (Memmert™ UN30,

Table 1
Parameters in the particle size distribution measurements.

Mineral	Flocculant concentration [g/t_{LCO}]	Flocculant
LCO-M	0, 10, 50	FO 4498
Graphite	0, 100	FO 4498

Table 2
The chemical parameters of the flotation experiments. Constant parameters, not listed in the Table, include a pulp density of 40 g/L, aeration rate of 2 L/min, pH of 5, and 8 ppm of MIBC (frother).

Experiment	Flocculant / concentration [g/ t_{LCO}]	Dispersant /concentration [g/ $t_{graphite}$]	Repetitions
1	None / "Pristine"	None	4
2	FO 4498 SSH / 10	None	6
3	FO 4498 SSH / 50	SHMP / 5000	1

Memmert, Schwabach, Bavaria, Germany) at 40 °C for 48 h. Figure 1 (reproduced from a previous work of the authors (Rinne et al., 2023)) shows a schematic representation of the experimental procedure.

2.3. Characterization of the froth products

2.3.1. X-ray fluorescence

The mass of dried froth concentrates and underflow fractions were measured in a laboratory scale, and the froth products characterized for their elemental composition with a portable X-ray fluorescence (XRF) gun (Oxford Instruments, X-MET 5000, Abingdon, United Kingdom). As the XRF gun could only analyze elements with atomic numbers ≥ 20, Co was used as a marker element for cathode particles. To transcribe the measured grade of Co into grades of LCO, and to improve the quantitative accuracy of the XRF analysis, calibration curves were obtained using reference mixtures of LCO and graphite with known compositions. The calibration curves are provided in *Fig.* S1 in the Supplementary Materials. Since the head grades and masses of both graphite and LCO in the model black mass were known, graphite grades were calculated from the LCO grade values and mass of froth fractions. The graphite content of the flotation underflow was then calculated based on mass balance, following a similar methodology as reported in the earlier study of the authors (Rinne et al., 2023).

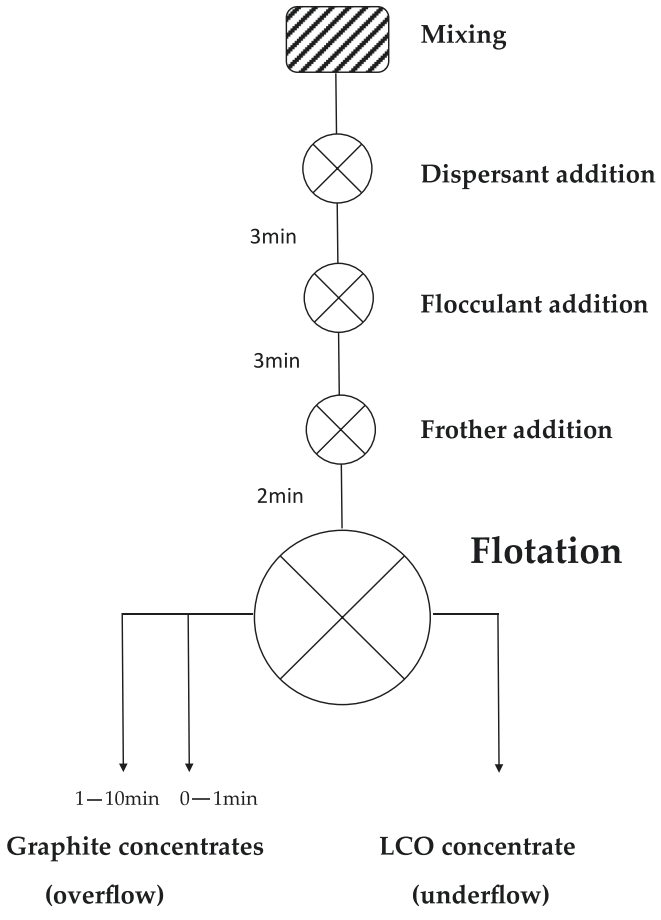

Fig. 1. A schematic representation of the flotation experiments.

2.3.2. Scanning electron microscopy

Concentrates from the flotation experiments were subjected to characterization with a scanning electron microscope (SEM) (Tescan Mira3, Brno, Czech Republic) to obtain images at different magnifications. The objective of the SEM analysis campaign was to determine whether evidence of floc formation could be detected within the graphite concentrate, which would indicate the formation of non-selective hydrophobic heteroflocs within the pulp.

It was presumed that, should flocs be detectable with SEM, they would appear as clustered particles of LCO within the graphite concentrate. To study this hypothesis, three types of flotation samples were prepared for SEM: i) graphite concentrate obtained with a pristine feed (control sample), to determine the amount of LCO clustering that happens naturally due to sample preparation (baseline clustering); ii) graphite concentrate obtained with a feed that was treated with excess concentration of flocculant (i.e., 50 g/t) hence promote heterofloc formation and providing a better chance at visualizing the clustered flocs within the sample; and iii) graphite concentrate obtained with a feed that was flocculated under conditions considered optimal (i.e., 10 g/t of flocculant), to study the selectivity of flocculation under said conditions.

The sample preparation for SEM was carried out immediately after froth products had been collected and dried. During preparation, the samples were carefully handled to avoid the influence of mechanical forces and prevent breakage of possible flock structures. Each sample was prepared by first applying an even layer of dried sample on a conductive carbon tape. Pressurized air was then applied to remove any sample that had not stuck to the tape. Acceleration voltage of 15 kV was selected for the studied graphite and lithium metal oxide samples (Friel, 2003) and images were obtained by mixing back-scattered electron and secondary electron signals to combine information regarding composition and particle morphology. Under these parameters, the relatively high atomic number Co in the LCO could be visualized as white particles that were easily distinguishable from the dark-colored particles of graphite.

2.3.3. Image processing

The SEM images obtained underwent analysis using public-domain software Fiji/Image J. The goal of the image analysis was to provide quantitative data on the clustering of the LCO particles within the froth samples, which could be regarded as evidence of flocculation as will be shown later in Section 3.3. A flow chart depicting the steps of the methodology hereby followed for image analysis and cluster identification is shown in Figure 2. The procedure can be divided into: i) preprocessing of the image(s); ii) identification of the cluster(s); and iii) categorizing the clusters into non-flocs and flocs.

Fig. 3 showcases a representative example of froth image processing sequence. Firstly, image segmentation was performed on the SEM image to identify all LCO particles. This was followed by feature extraction where spatial coordinates and area of each individual LCO particle were determined. This procedure was adopted for a total of 75 images obtained through SEM with magnification of 500x. The obtained features were used as input to a machine learning algorithm (DBSCAN) aimed at identifying clusters and patterns within the data. DBSCAN algorithm requires two input parameters: Epsilon (Eps); and Minimum Points (MinPts), to identify clusters. Eps is defined as the radius within which nearby points are part of clusters whereas MinPts sets the minimum number of neighboring points within the Eps radius to constitute them as cluster points. The integration of these two parameters facilitates the formation of density-based clusters and enables the classification of each point within a cluster as a core point, border point, or noise point. Core points represents data points located in dense regions and satisfy the

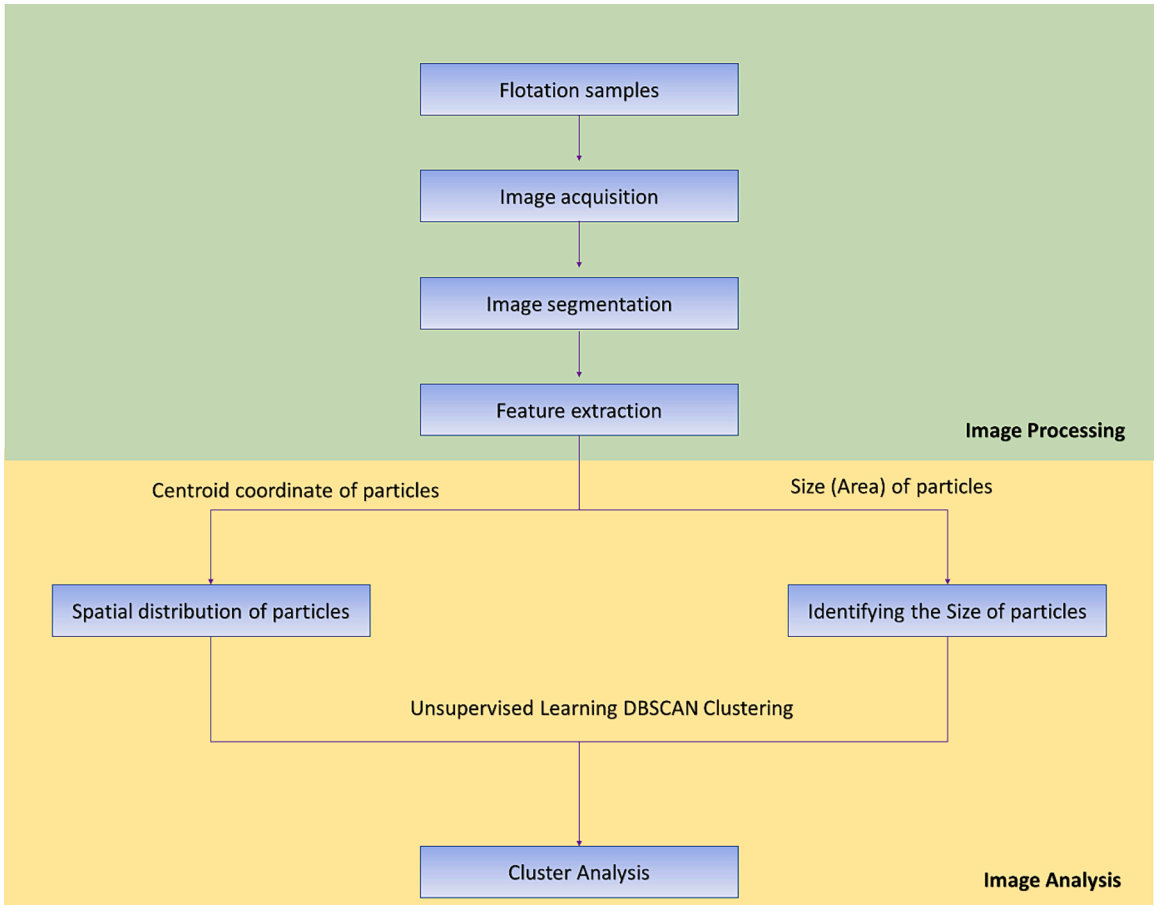

Fig. 2. The flowchart for image processing and cluster analysis.

MinPts condition within a specified Eps radius. Border points on the other hand reside at the edges of clusters, but do not meet MinPts requirement. Noise points, or outliers, fail to meet the criteria for neither Epsilon nor MinPts. Distinguishing between these types of points enables DBSCAN to capture the density-based structure of data, identifying clusters while accommodating irregular shapes and dispersed data. Accordingly, only clustered particles that would satisfy the chosen Eps and MinPts requirements would be considered as flocs for the purposes of this article.

The SEM data obtained in this study exhibited extensive dispersion and irregular distribution of LCO particles. Consequently, DBSCAN was chosen as the core processing algorithm to analyze the data and explore underlying clusters. R-studio 2022.07.1 + 554 software was used to run DBSCAN algorithm and categorize various clusters as either flocs or non-flocs. We selected SEM images taken from a non-flocculated control sample and conducted multiple iterations to ultimately determine the value of Eps as 23 μm, and MinPts as 10. Under these parameters, the number of false positive results (baseline clusters identified as flocs) was satisfyingly low, as will be later shown in Section 3.3. The iteration process applied to determine the DBSCAN parameters is further discussed in the Supplementary Materials.

3. Results and discussions

3.1. Particle size distributions

PSDs of graphite and LCO in a pulp pH of 5 are shown in Figure 4 for both pristine and flocculated samples.

The results shown in Fig. 4 suggest that a cationic flocculant can reduce the presence of ultrafine LCO particles (i.e., <10 μm) as a function of its concentration – a result in-line with previously published data (Rinne et al., 2023). Admittedly, the change in the ultrafine particle count of the LCO sample is very subtle, especially with the lower flocculant concentration of 10 g/t. Therefore, only minor improvements in flotation performance can be expected, even if flocculation of model black mass mixtures was selective under said concentration.

Figure 4 also shows that dispersions of pure graphite do not respond to the flocculant, as the PSD stays virtually unaffected even when conditioned with a relatively high flocculant concentration of 100 g/t. This corroborates the behavior previously reported by our research group (Rinne et al., 2023), and supports the hypothesis that flocculation selectivity in mixed mineral black mass dispersions can be achieved. In practice, selective flocculation is not trivial and previous research has provided indirect evidence that flocculation selectivity is lost above certain concentration limit (Rinne et al., 2023).

In addition to PSD measurements, jar tests were performed by measuring the speed of sedimentation of non-flocculated and flocculated suspensions under a relatively high 100 g/t flocculant concentration. The results of the jar tests are provided in Fig. S4 in the Supplementary Materials.

3.2. Scanning electron microscopy images of froth samples

Firstly, a control sample obtained by floating a black mass in the absence of flocculant was subjected to SEM. The sample was carefully scanned for clustered particles of LCO. Representative SEM images of the control sample are shown in Figure 5.

The SEM images show that LCO clusters in the 0–1 min froth fraction of the control sample were infrequent and only a few individual particles reported to samples of the concentrates. Closeups of such particles can

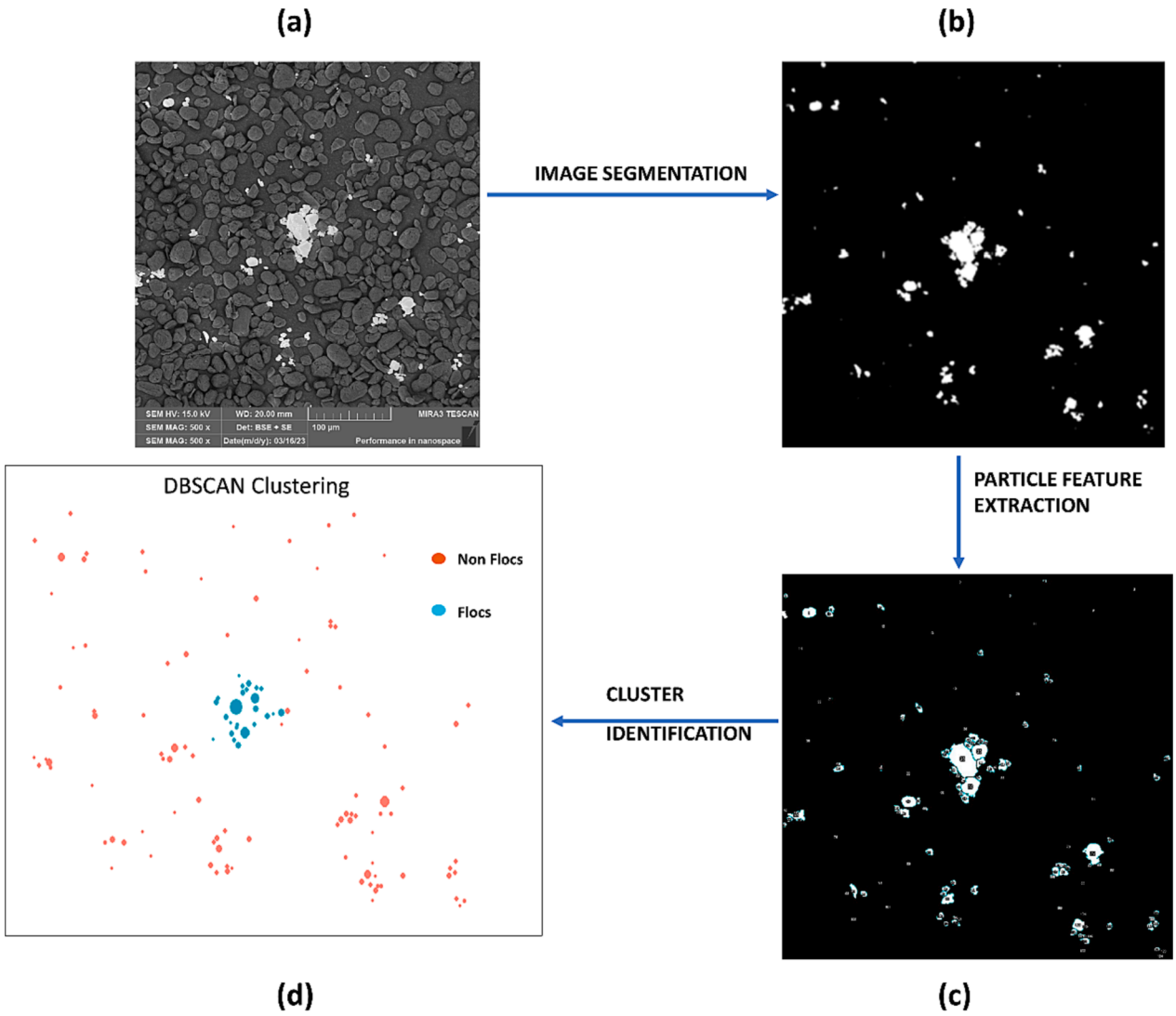

Fig. 3. (a) SEM image, (b) image segmentation, (c) feature extraction and (d) DBSCAN clustering.

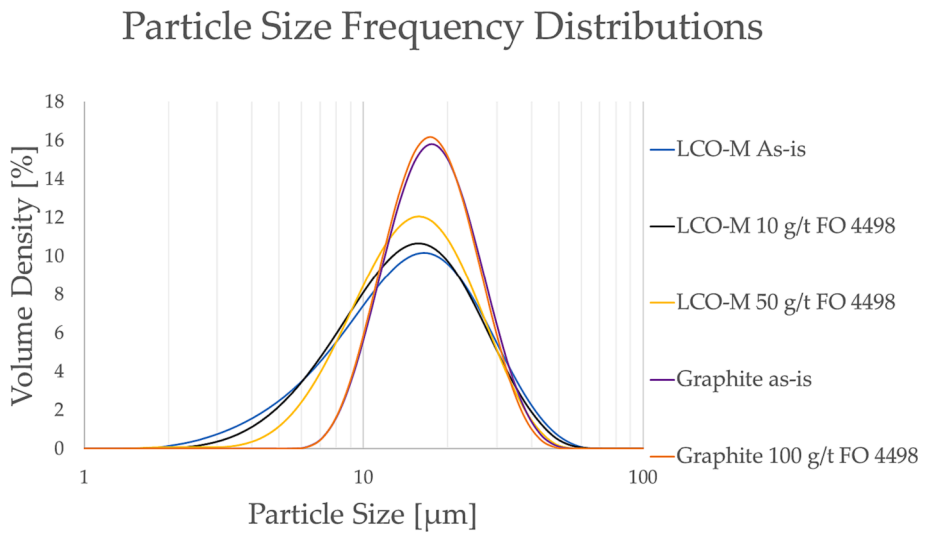

Fig. 4. Particle size frequency distributions of graphite and LCO samples, applying various concentrations of the FO 4498 flocculant.

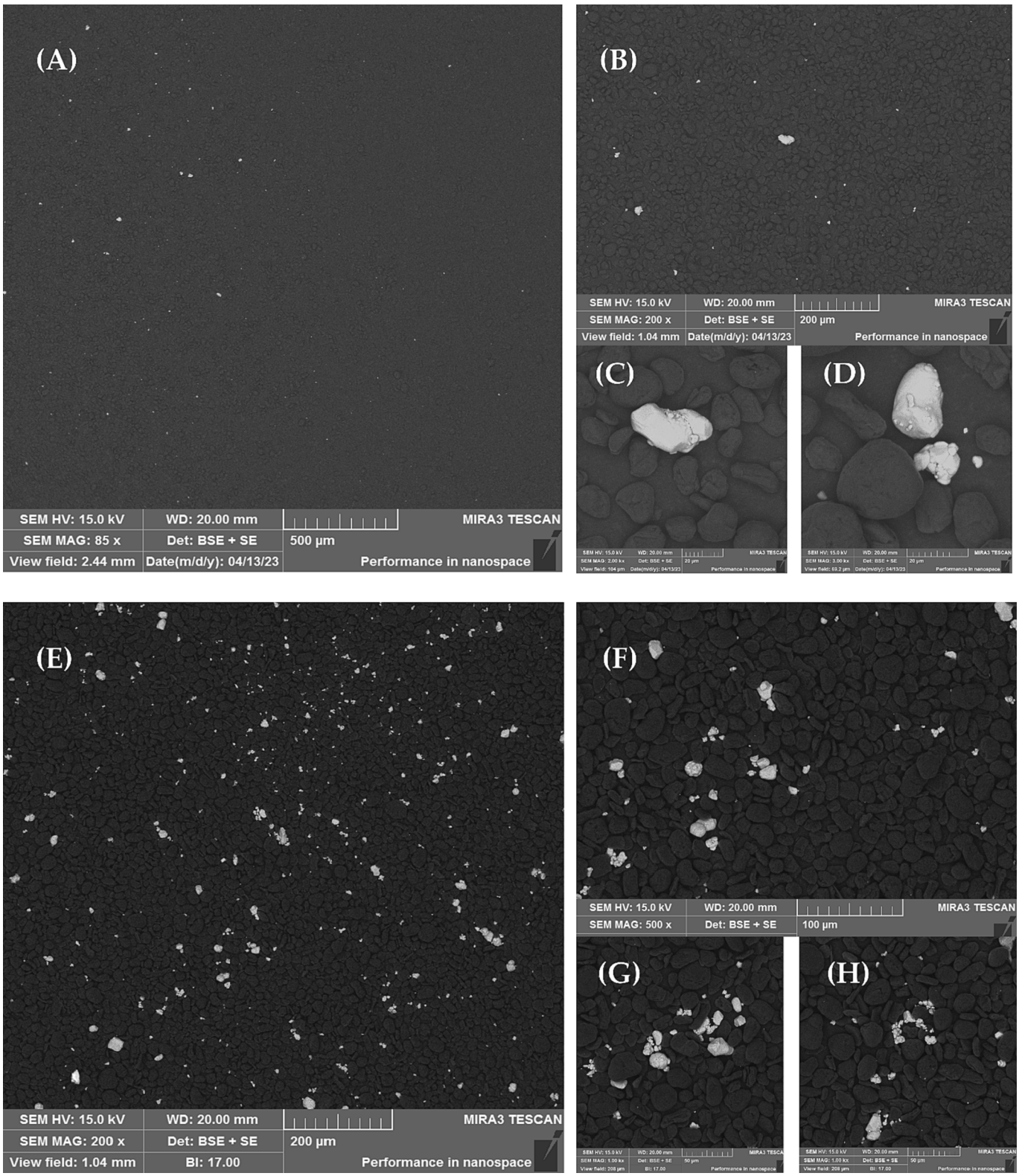

Fig. 5. SEM images of the flotation products of model black mass in the absence of flocculant. Figures (A)-(D) taken from the 0–1 min concentrate, (E)-(H) from the 1–10 min concentrate.

be seen in Fig. 5*(C), and (D)*. The concentration of LCO in the 1–10 min froth concentrate would increase significantly compared to 0–1 min fraction, which is clearly visualized in the 200x low-magnification SEM image provided in Fig. 5*(E)*. In order to reliably identify flocs in the flocculated froth samples later on, it is necessary to map out the cluster characteristics of the LCO particles in the 1–10 min froth concentrates, in which the higher LCO content would naturally lead to increased rate of clustering by chance (baseline clustering). Representative close-up images of such baseline clusters are shown in Fig. 5(F, G, and H). The baseline clusters are found to be non-continuous (obstructed by graphite

particles), and with a relatively small population (<10 particles).

The second SEM sample was obtained from flotation of model black mass conditioned with flocculant in excess concentration (i.e., 50 g/t), which was suspected to result in the formation of hydrophobic heteroflocs based on the grade-recovery data presented in an earlier article of the authors (Rinne et al., 2023). Representative SEM images of this sample are shown in Figure 6.

As seen in Fig. 6*(A)*, the 0–1 min concentrate of the excessively flocculated sample contains a relatively high amount of LCO particles compared to the *pristine* black mass (Fig. 5(A, B)). Interestingly, closeup images reveal many LCO clusters within the sample, exemplified in Fig. 6 (B, C, and D). These clusters are continuous (unobstructed by graphite particles), which is a characterizing feature compared to the baseline clusters found in the control sample (Fig. 5(F, G, H)). The clusters can be regarded as indirect evidence that the LCO particles have been transported into the froth as a part of a flocculated structure. Since the commonly accepted principles of flotation would suggest that flocculated LCO is unlikely to undergo entrainment due to their large size, a reasonable deduction is that the graphite particles in the vicinity of the cluster were also part of the floc. Such heteroflocculation would provide the means for true flotation of the floc.

Lastly, SEM images of the graphite concentrate obtained by flocculating the black mass under optimal concentration of flocculant (i.e., 10 g/t) are shown in Figure 7. As seen, no particle clusters are found within the 0–1 min froth concentrates. Furthermore, the absence of bright-colored particles in the lower magnification images in Fig. 7(A, B) already suggest the production of graphite with high purity. These images indicate that, if flocculation happens under these conditions, no heteroflocs are recovered during the first minute of separation.

As flotation experiment progresses, a larger number of LCO particles are detected Fig. 7(F-I), although clusters are infrequent, and mostly consist of low number of particles that cannot be reliably identified as flocs (Fig. 7(G, H)). That being said, some LCO clusters were found, such as the one pictured in Fig. 7*(E)*. This cluster shares similarities with the ones observed in the sample with excess flocculant (Fig. 6(B-D)), as multiple LCO particles form an unobstructed continuous structure. This provides evidence that flocculation of LCO occurs under these conditions, but the heteroflocculation promoting their flotation is less common. To objectively study the frequency of heteroflocs in the optimally flocculated sample, image processing was utilized, as described in the next Section 3.3.

3.3. Image processing for floc structure characterization

Each SEM image acquired from the froth samples was subjected to image analysis via a DBSCAN algorithm to quantify the amount of clustered LCO particles that could be reliably identified as flocs. Earlier in Section 2.3.3 (Fig. 3), a demonstration of cluster identification was provided for the particle shown in Fig. 6 (B). The compiled results of image analysis are presented in Table 3.

As shown in Table 3, out of 49 images taken of pristine froth concentrates, only one LCO cluster was identified as a floc. In comparison, the excessively flocculated samples (50 g/t) contain 25 flocs within 26 images analyzed. The floc observed in the pristine sample can be viewed as an anomaly, showcasing that the chosen image analysis protocol produces a reasonably low count of false positives, and is therefore suitable for detection of flocs. This observation also provides further evidence for the loss of flocculation selectivity when a flocculant is applied in excess.

Perhaps the most intriguing deductions can be drawn from the image analysis results of the optimally flocculated froth samples. In these samples, out of 22 images analyzed, no flocs are identified within the 0–1 min froth concentrates. It is thus highly probable that the recovery of flocs in froth is prevented during the first minute of the experiment, which supports the results published in an earlier work of the authors (Rinne et al., 2023). In the 1–10 min samples, 8 flocs are identified in a total of 25 images analyzed. This suggests that some LCO-graphite heteroflocs can be formed even under low flocculant concentrations, and

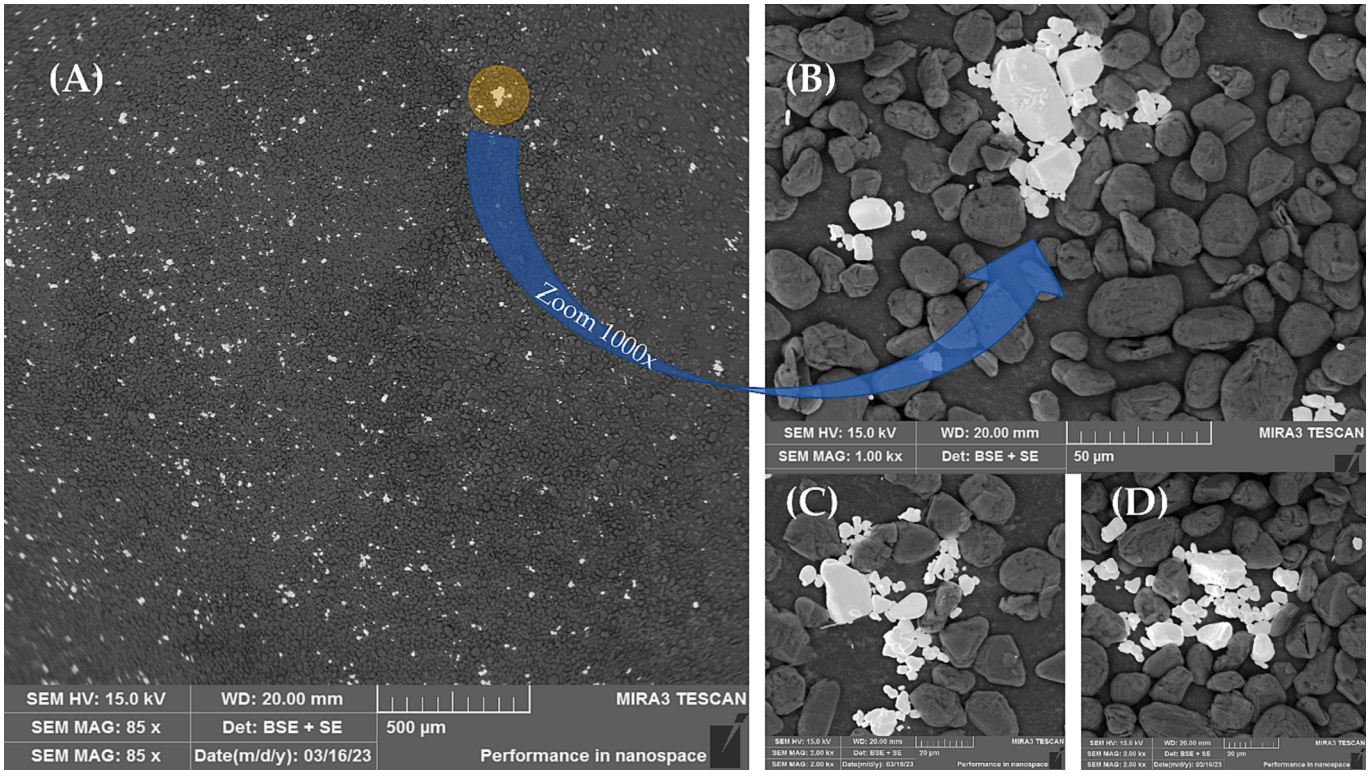

Fig. 6. SEM images of the flotation (LCO-M + graphite) froth samples conditioned with excess flocculant concentration. Images (A)-(D) all taken from the 0–1 min concentrate.

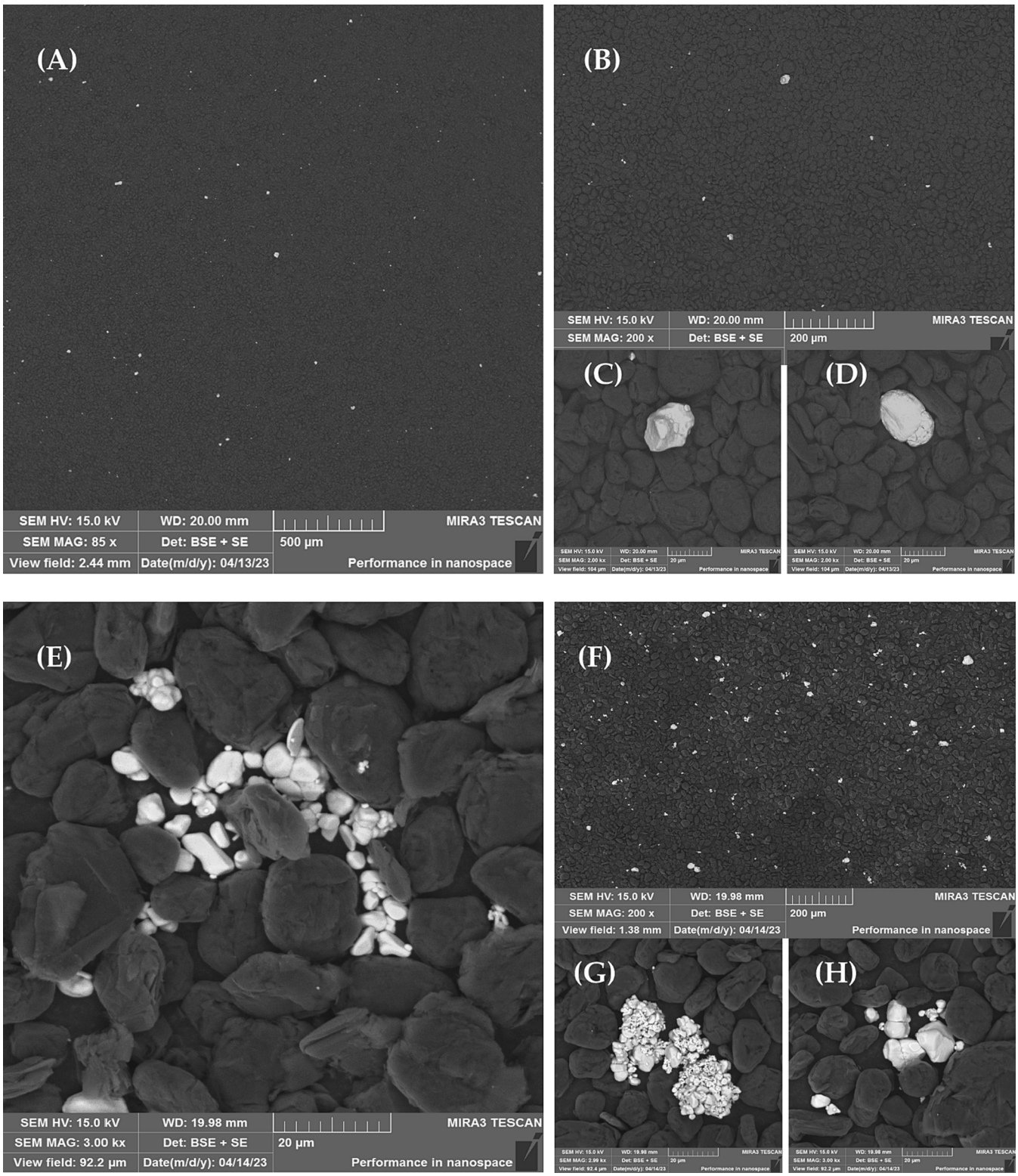

Fig. 7. SEM images of flotation products of model black mass conditioned with optimal flocculant concentration. Figures (A)-(D) taken from the 0–1 min concentrate, (E)-(H) from the 1–10 min concentrate.

that some of them are hydrophobic enough to be eventually recovered in the concentrate. Their presence at the later stage in flotation supports the hypothesis that a difference in the degree of hydrophobicity of heteroflocs vs. free graphite particles results in distinctive separation kinetics, allowing for the comparatively more hydrophobic free graphite particles to be recovered first. In practice, this means that even in the case where flocculation selectivity is partially lost, high grades of graphite can be obtained by controlling residence time.

3.4. Flotation experiments

The grade-recovery curves for graphite concentrates obtained after

Table 3
Image analysis results indicating the number of clusters identified as flocs within the flotation concentrates.

Flocculant concentration / concentrate	Number of Images Analyzed	Number of Clusters Identified as Flocs
Pristine / 0–1 min	25	0
Pristine / 1–10 min	24	1
50 g/t / 0–1 min	5	5
50 g/t / 1–10 min	21	20
10 g/t / 0–1 min	22	0
10 g/t / 1–10 min	25	8

the flotation experiments are found in Figure 8.

Fig. 8*(A)*, shows the grade-recovery curves obtained in the absence of flocculant in comparison with a sample that has been flocculated using 50 g/ton FO 4498. A significant drop in the grade of the graphite concentrate is observed when the flocculant is applied in such excess concentration, whereas the recovery stays virtually unaffected. The presented data further confirms that hydrophobic heteroflocs are produced in the excessively flocculated system, which results in true flotation of entrapped LCO. This finding is well aligned with the SEM results earlier shown in Fig. 6 (A-D).

From Fig. 8*(A)*, a comparison between the pristine medium-sized LCO-M sample can be made to the results published in an earlier work, in which model black masses with comparatively coarser and finer LCOs were subjected to flotation (Rinne et al., 2023). When comparing the graphite grades of the 0–1 min concentrates, 99.4 %, 98.8 %, and 98.2 % grades are achieved in an order of descending LCO particle size. Cumulative graphite grades at the end of experiments were 98.9 %, 98.1 %, and 97.7 %, respectively. The cumulative recovery of graphite was similar in all of the experiments (97.6 %-98.4 %). As highlighted by these results, entrainment of ultrafine cathode particles seems to prevent recovering the graphite at an acceptable grade (i.e., 99 %), even from a fully liberated and binder-free model black mass. In the case of the coarse sample however, battery-grade graphite (99.4 % pure) graphite is recovered during the first minute. Cathode particle size control via selective flocculation might therefore be necessary for the economic recovery of waste LIB graphite.

Fig. 8*(B)* compares the average grade-recoveries of graphite in the absence and presence of flocculant with a concentration of 10 g/t, including one standard deviation of error for the grade value. In the flocculated feed, an average graphite grade of 98.9 % is recorded at the 1 min mark, compared to an average grade of 98.8 % in the pristine system. The average cumulative graphite grades at the end of experiment were observed to be 98.2 %, and 98.1 %, respectively. This minor, albeit consistent difference in the graphite grades could be reasonably explained by the decreased entrainment of selectively flocculated LCO particles. Admittedly, due to the limited resolution of macroscopic batch flotation tests, a statistically meaningful confirmation of this hypothesis cannot be made based on the grade-recovery measurements. As seen in Fig. 8 (**B**), these differences are well within experimental error. However, this behavior is supported by the SEM (Fig. 7(A, B)) and image processing results (Table 3), where no evidence of flocculated LCO being recovered in the froth concentrate during the first minute of separation was found, and only a few flocs were recovered during later stages of the experiment, in the optimally flocculated sample. These findings corroborate that no large-scale loss of flocculation selectivity takes place when applying a flocculant dosage of 10 g/t.

An important distinction to previously published results (Rinne et al., 2023) is that the separation kinetics do not seem to be affected by flocculation, as the cumulative recovery of graphite at 1 min and 10 min mark is similar with both flocculated and pristine black mass (Fig. 8(A, B)). In contrast, the work published earlier showed that graphite recovery at 1 min dropped significantly in the presence of a flocculant. The improved separation kinetics are presumably a result of the careful pH control throughout the experiment. According to the zeta potential data published in earlier work of the authors (Rinne et al., 2023), when pH is kept at 5–6, graphite surfaces remain electrically neutral enough to not be affected by a cationic flocculant at low concentrations.

4. Conclusions

SEM was successfully applied to study flotation concentrates recovered from LCO-graphite model black mass, providing visual evidence of the formation of LCO particle clusters, indicating heteroflocculation with graphite. Furthermore, DBSCAN machine learning algorithm was developed and applied to provide a quantitative and objective analysis of the SEM results. Under optimal flocculant concentration of 10 g/t, only a few flocs were detected in the froth concentrate, which suggested that large-scale heteroflocculation is avoided under said conditions. Higher flocculant concentration (50 g/t) resulted in flocculated LCO particles commonly reporting to the froth, signaling a loss of flocculation selectivity. The presence of flocs in the dried froth products indicates that the flocs in the studied colloidal system possess sufficient mechanical integrity to withstand the hydrodynamic forces present in a flotation cell. The results showed that SEM imaging combined with DBSCAN analysis can be applied as a novel method for detecting evidence of heteroflocculation in flotation pulps/froths, and to determine the degree of selectivity in a process that applies selective flocculation as a conditioning stage for froth flotation.

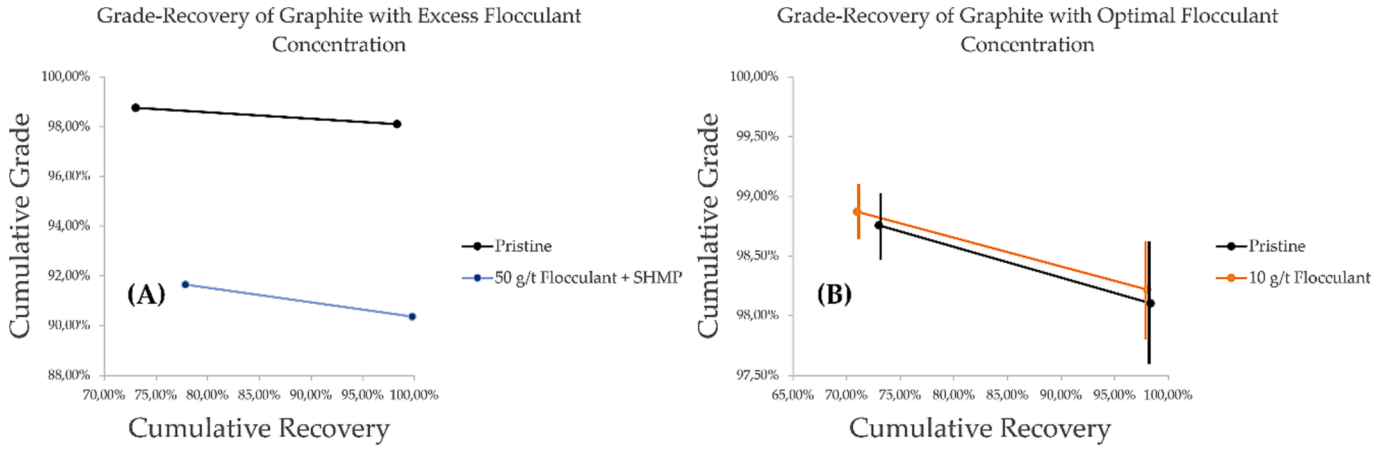

Fig. 8. Grade-recovery curves for graphite in the flotation experiments. (A) Mean values for experiments with a pristine black mass feed compared to a feed prepared with 50 g/t flocculant, (B) Mean values for experiments with 10 g/t flocculant concentration compared to the mean values of pristine experiments, including one standard deviation above and below the mean for the grade value.

Proper pH control before and during flotation seemed to prevent the kinetics of separation from being negatively influenced by flocculation, as had been reported in earlier research (Rinne et al., 2023). These findings verify that using relatively low flocculant dosages, alongside pH control within the range of 5–6, can help avoid bulk heteroflocculation of LCO and graphite. The increment of graphite grade in the flocculated system could be reasonably explained by the selectively flocculated LCO particles being less prone to entrainment. However, it is crucial to acknowledge that due to the limited resolution of batch flotation tests, statistically significant conclusions regarding the impact of selective flocculation on flotation performance could not be drawn. The results however suggest that selective flocculation is a potential method to increase the separation efficiency of graphite from LIB black mass.

Conditioning the flotation pulp with an excess amount of flocculant however resulted in clear non-selective adsorption on the graphite surfaces, leading to the formation of LCO-graphite heteroflocs, and increasing the recovery of LCO to the froth via entrapment. Indeed, with a flocculant concentration of 50 g/t the grade of graphite concentrate was decreased. These results corroborate the findings of the SEM characterization campaign. Under the conditions used in this study, SHMP dispersant did not shield the graphite from heteroflocculating with LCO under moderate (50 g/t) flocculant concentrations, even though it was previously reported to positively influence flocculation selectivity under low flocculant concentrations of 20 g/t (Rinne et al., 2023).

The results hereby presented open multiple avenues for further research. Firstly, studying the mechanical parameters of flocculant conditioning is of interest since agitation rate and residence time have been reported to influence floc formation and growth. Furthermore, research should be prolonged to encompass other parameters effecting flotation performance such as by exploring hydrodynamic parameters as demonstrated by (Saeed et al., 2022). In the context of black mass flocculation-flotation, additional cathode chemistries should be studied to better mimic the conditions of battery recycling found in industry, in which presorting by cathode chemistry is not a common practice. Additionally, means for preventing graphite heteroflocculation are needed to fully unlock the potential of selective flocculation. Finding graphite selective dispersants, or active-site blocking agents, could allow the use of higher flocculant dosages and a more efficient agglomeration of LCO particles.

CRediT authorship contribution statement

Tommi Rinne: Writing – original draft, Methodology, Investigation, Conceptualization. **Mohazzam Saeed:** Writing – original draft, Investigation, Data curation. **Rodrigo Serna-Guerrero:** Writing – review & editing, Supervision, Project administration, Funding acquisition.

Declaration of competing interest

The authors declare that they have no known competing financial interests or personal relationships that could have appeared to influence the work reported in this paper.

Data availability

Data will be made available on request.

Acknowledgments

This research work was funded by Business Finland BATCircle 2.0 project, grant number 44886/31/2020. The authors thank Dr. Hanna Sahivirta for providing her help on SEM-EDS characterization.

Appendix A. Supplementary data

Supplementary data to this article can be found online at https://doi.org/10.1016/j.mineng.2024.108644.

References

Beaudet, A., Larouche, F., Amouzegar, K., Bouchard, P., Zaghib, K., 2020. Key challenges and opportunities for recycling electric vehicle battery materials. Sustainability 12 (14), 5837.
Brückner, L., Frank, J., Elwert, T., 2020. Industrial recycling of lithium-ion batteries—a critical review of metallurgical process routes. Metals 10 (8), 1107.
Chen, Z., Zhang, W., Yang, Z., 2019. A review on cathode materials for advanced lithium ion batteries: microstructure designs and performance regulations. Nanotechnology 31 (1), 012001.
Cheng, K., Wu, X., Tang, H., Zeng, Y., 2022. The flotation of fine hematite by selective flocculation using sodium polyacrylate. Miner. Eng. 176, 107273 https://doi.org/10.1016/j.mineng.2021.107273.
Dańczak, A., Ruismäki, R., Rinne, T., Klemettinen, L., O'Brien, H., Taskinen, P., Jokilaakso, A., Serna-Guerrero, R., 2021. Worth from waste: utilizing a graphite-rich fraction from spent lithium-ion batteries as alternative reductant in nickel slag cleaning. Minerals 11 (7), 784.
Ester, M., Kriegel, H. P., Sander, J., Xiaowei, X. 1996. A density-based algorithm for discovering clusters in large spatial databases with noise. Proceedings of the Second International Conference on Knowledge Discovery and Data Mining, pp. 226–231.
Folayan, T.-O., Lipson, A.L., Durham, J.L., Pinegar, H., Liu, D., Pan, L., 2021. Direct recycling of blended cathode materials by froth flotation. Energ. Technol. 9 (10), 2100468.
Friel, J.J., 2003. X-ray and image analysis in electron microscopy, 2nd edn. Princeton Gamma-Tech. Inc., Princeton, NJ.
Harper, G., Sommerville, R., Kendrick, E., Driscoll, L., Slater, P., Stolkin, R., Walton, A., Christensen, P., Heidrich, O., Lambert, S., 2019. Recycling lithium-ion batteries from electric vehicles. Nature 575 (7781), 75–86.
He, Y., Zhang, T., Wang, F., Zhang, G., Zhang, W., Wang, J., 2017. Recovery of LiCoO2 and graphite from spent lithium-ion batteries by Fenton reagent-assisted flotation. J. Clean. Prod. 143, 319–325.
Huang, Y., Han, G., Liu, J., Chai, W., Wang, W., Yang, S., Su, S., 2016a. A stepwise recovery of metals from hybrid cathodes of spent Li-ion batteries with leaching-flotation-precipitation process. J. Power Sources 325, 555–564.
Huang, Y., Han, G., Liu, J., Wang, W., 2016b. A facile disposal of Bayer red mud based on selective flocculation desliming with organic humics. J. Hazard. Mater. 301, 46–55.
Kumar, R., Mandre, N.R., 2017. Selective flocculation of low grade iron ore slimes using different types of polymers. Indian J. Chem. Technol. 24, 411–416.
Li, X., 2022. Selective flocculation performance of amphiphilic quaternary ammonium salt in kaolin and bentonite suspensions. Colloids Surf A Physicochem Eng Asp 636, 128140.
Li, M., Xiang, Y., Chen, T., Gao, X., Liu, Q., 2021. Separation of ultra-fine hematite and quartz particles using asynchronous flocculation flotation. Miner. Eng. 164, 106817.
Liu, J., Wang, H., Hu, T., Bai, X., Wang, S., Xie, W., Hao, J., He, Y., 2020. Recovery of LiCoO2 and graphite from spent lithium-ion batteries by cryogenic grinding and froth flotation. Miner. Eng. 148, 106223.
Mu, C., Hou, Y., Zhao, J., Wei, S., Wu, Y., 2023. Stream-DBSCAN: A streaming distributed clustering model for water quality monitoring. Appl. Sci. 13 (9), 5408.
Rinne, T., Klemettinen, A., Klemettinen, L., Ruismäki, R., O'Brien, H., Jokilaakso, A., Serna-Guerrero, R., 2022. Recovering value from end-of-life batteries by integrating froth flotation and pyrometallurgical copper-slag cleaning. Metals 12 (1), 15.
Rinne, T., Araya-Gómez, N., Serna-Guerrero, R., 2023. A study on the effect of particle size on li-ion battery recycling via flotation and perspectives on selective flocculation. Batteries 9 (2), 68.
Ruismäki, R., Rinne, T., Dańczak, A., Taskinen, P., Serna-Guerrero, R., Jokilaakso, A., 2020. Integrating flotation and pyrometallurgy for recovering graphite and valuable metals from battery scrap. Metals 10 (5), 680.
Saeed, M., De Souza, C.V., Chipakwe, V., Chelgani, S.C., 2022. Influence of hydrodynamic variables on scaling up of mechanical flotation cells. Arab. J. Geosci. 15 (20), 1606. https://doi.org/10.1007/s12517-022-10908-7.
Salces, A.M., Bremerstein, I., Rudolph, M., Vanderbruggen, A., 2022. Joint recovery of graphite and lithium metal oxides from spent lithium-ion batteries using froth flotation and investigation on process water re-use. Miner. Eng. 184, 107670.
Saneie, R., Abdollahi, H., Ghassa, S., Azizi, D., Chehreh Chelgani, S., 2022. Recovery of copper and aluminum from spent lithium-ion batteries by froth flotation: a sustainable approach. Journal of Sustainable Metallurgy 8 (1), 386–397.
Traore, N., Kelebek, S., 2022. Characteristics of spent lithium ion batteries and their recycling potential using flotation separation: A review. Miner. Process. Extr. Metall. Rev. 1–29.
Vanderbruggen, A., Gugala, E., Blannin, R., Bachmann, K., Serna-Guerrero, R., Rudolph, M., 2021. Automated mineralogy as a novel approach for the compositional and textural characterization of spent lithium-ion batteries. Miner. Eng. 169, 106924 https://doi.org/10.1016/j.mineng.2021.106924.
Vanderbruggen, A., Salces, A., Ferreira, A., Rudolph, M., Serna-Guerrero, R., 2022. Improving separation efficiency in end-of-life lithium-ion batteries flotation using attrition pre-treatment. Minerals 12 (1), 72.
Velázquez-Martínez, O., Valio, J., Santasalo-Aarnio, A., Reuter, M., Serna-Guerrero, R., 2019. A critical review of lithium-ion battery recycling processes from a circular economy perspective. Batteries 5 (4), 68.
Wang, C., Sun, C., Liu, Q., 2021a. Entrainment of gangue minerals in froth flotation: mechanisms, models, controlling factors, and abatement techniques—a review. Mining, Metallurgy & Exploration 38, 673–692.

Wang, C., Wang, P., Tan, X., Huang, G., Kou, J., Sun, C., Liu, Q., 2021b. Selective aggregation of fine quartz by polyaluminum chloride to mitigate its entrainment during fine and ultrafine mineral flotation. Sep. Purif. Technol. 279, 119606.
Yu, J., He, Y., Ge, Z., Li, H., Xie, W., Wang, S., 2018. A promising physical method for recovery of LiCoO2 and graphite from spent lithium-ion batteries: Grinding flotation. Sep. Purif. Technol. 190, 45–52.
Zhang, G., Ding, L., Yuan, X., He, Y., Wang, H., He, J., 2021. Recycling of electrode materials from spent lithium-ion battery by pyrolysis-assisted flotation. J. Environ. Chem. Eng. 9 (6), 106777.